SURROGATE MODEL FOR THIRD-INTEGER RESONANCE EXTRACTION AT THE FERMILAB DELIVERY RING*

A. Narayanan[†], J. Berlioz, K. Danison-Fieldhouse, K. Hazelwood, M. Khan,
J. St. John, N. Tran, A. Whitbeck, Fermilab, Batavia, IL, USA
J. Ji, M. Walter, Toyota Technical Institute of Chicago, Chicago, IL, USA

Abstract

We present an ongoing work in which a surrogate model is being developed to reproduce the response dynamics of the third-integer resonant extraction process in the Delivery Ring (DR) at Fermilab. This effort is in pursuit of smoothly extracting circulating beam to the Mu2e Experiment's production target, wherein the goal is to extract a uniform slice of the circulating $1e12$ protons in the DR over 25,000 turns (43 ms). The DR contains 3 harmonic sextupoles which excite a third-integer resonance as well as three fast, tune-ramping quadrupole magnets which drive the horizontal tune towards the $29/3$ resonance. In our initial work the surrogate model trains on a semi-analytical simulation provided in the same format as live data. Using Reinforcement Learning (and other potential ML methods), the trained surrogate acts as the "environment" in which a simple ML control agent could learn to dynamically adjust the quadrupole ramp at 430 break points within the 43 microsecond spill window. The control agent will be hosted on a dedicated Arria 10 FPGA, introducing its own requirements on control agent architecture. In this work we report the accuracy and fidelity of surrogate models in comparison to the response dynamics of the physics simulator.

THE MU2E EXPERIMENT AND BEAM REQUIREMENT

Mu2e is an upcoming experiment [1] at Fermi National Accelerator Laboratory (Fermilab) that intends to look for beyond-standard-model (BSM) physics through charged lepton flavor violation. Mu2e will heavily suppress large systematic effects such as RPC background [2] by using a pulsed muon beam (from a pulsed proton beam) and delaying the detector live window, enabling a clean measurement of muon-converted electrons.

The pulsed proton beam (see Table 1) (directed to the muon production target) will be produced using a third-integer resonant extraction process at Fermilab's Delivery Ring (DR). The goal is to inject $1e12$ protons into the DR and uniformly extract equal slices of the circulating proton beam, sending these micropulses to the production target. A Spill Regulation System (SRS) [3] is commissioning in order to facilitate the uniformity of the spill by achieving a Spill Duty Factor (SDF) of 60% or greater.

Table 1: Some Main Parameters Pertinent to Resonant Extraction

Parameter	Value
Beam kinetic energy	8 GeV
Spill Duration	43 ms
Number of spills per super cycle	8
Number of bunches per spill	1
Initial proton intensity	10^{12} protons
# of protons extracted per turn	$< 4 \times 10^7$ protons
Time between proton micropulses	1.695 µs
Normalized Emittance (95%) ϵ_x	16 π mm-mrad
Spill Duty Factor (SDF)	$> 60\%$
Reset time between spills	5 ms

PHYSICS ENVIRONMENT

To simulate the 3rd integer resonant extraction, the most accurate choice of simulation would be to perform particle tracking. However, even simulating an intensity of 1e12 protons with 1e7 macroparticles over 25,000 turns would be very computationally expensive. A semi-analytical model was built to simulate of the 3rd integer resonant extraction, consisting of following components.

Noise in spill rate The modeling of the spill, for the purposes of Fast Regulation, assumes a *perfect* extraction in the absence of any instantaneous noises in the system, with the assumption that a logarithmic quad ramp curve would result in ideal extraction rate. The physics simulator generates random log-normal points at 1 kHz rate and interpolates the generated points to provide smooth noise data for over 430 time steps (since the maximum SRS design bandwidth is 10 kHz), with each time step constituting 100 µs (or equivalently ≈60 turns). The expectation value of the spill rate is normalized to 1, and the log-normal generated noise is added to 1 to give us a noise profile for every spill.

PID Control Loop Once the noise in the spill rate is generated, and the error in the spill rate known, it is sequentially fed to the PID control loop, with the three gain values of the PID controller passed as an argument. The PID function inputs the gain values, the spill rate data, and computes the control signal for each of the time steps, given by Eq. (1):

$$u(t) = G_p e(t) + G_I \int_0^t e(\tau)\, \mathrm{d}\tau + G_d \frac{\mathrm{d}}{\mathrm{d}t} e(t), \quad (1)$$

6th North American Particle Accel. Conf. (NAPAC2025), Sacramento, CA, USA   JACoW Publishing

ISBN: 978-3-95450-261-5   ISSN: 2673-7000   doi: 10.18429/JACoW-NAPAC2025-MOP089

where G_p, G_i, G_d are the proportional, integral, and derivative gains. In this modeling of the PID controller we do not incorporate a low-pass filter within the derivative action of the controller since the generated noise is guaranteed to not have any divergence in $de(t)/dt$.

B-Field Shielding Effect   High-frequency corrections from the PID to the quadrupole power supplies produce rapidly varying B-fields that are screened by the stainless-steel beam pipe and therefore do not reach the beam; we model this shielding with a Butterworth low-pass filter (1 kHz cutoff).

Transit-Time Delay   Once the horizontal tune of the beam is changed by the fast tune-shifting quadrupoles, the particles take a finite amount of time (nonzero orbit count) to be extracted due to the non-linear beam dynamics, called a 'transit time' delay, which is incorporated into the model.

Quadrupole Response and Beam Extraction   The control signal is then passed through a function that superposes it to the predefined logarithmic ideal quad current ramp value. The ideal-spill resulting quad current was taken to be a logarithmic function of the spill timestep, with a maximum current value of 100 A. Once we have the total extracted beam intensity for every time step, we can calculate the rate of spill intensity, which is obtained from a resistive wall monitor in the extraction line. The spill monitor function computes the difference in the total spill intensity from the j-th time step to the $(j+1)$-th time step, ideally zero. The spill monitor thus outputs the *regulated* extraction rate, which is the final output of the physics simulator.

REPRODUCING PHYSICS SIMULATOR DYNAMICS IN SURROGATE MODELS

Training Procedures

To reproduce surrogate dynamics, we train models on histories of spill intensities represented as state-action pairs (s_t, a_t), where $a_t \in \mathbb{R}^2$ encodes the corrected quadrupole current and PID control action. Given a sequence $\{(s_{t-N}, a_{t-N}), \dots, (s_t, a_t)\}$, the model is tasked with predicting the next spill intensity s_{t+1}. We initially use teacher forcing [4], conditioning on simulator generated histories during training. Our model predicts a horizon of 10 steps $\{s_{t+1}, \dots, s_{t+10}\}$, using the first step as the predicted spill s_{t+1}. This allows longer-horizon learning while remaining compatible with our 10-step interpolation.

To mitigate exposure bias, we then use teacher-based weaning, a variant of scheduled sampling [5], reducing simulator generated inputs by 5 every 10 epochs ($20{\rightarrow}15{\rightarrow}10{\rightarrow}5{\rightarrow}0$), and correspondingly increasing surrogate generated inputs by 5. This gradual shift from supervised to autoregressive inference improves robustness to compounding errors.

Model

Because the spill rate varies stochastically, we adopt a variational surrogate model [6] to better capture its dynamics. For both training strategies, training is performed on sliding windows of length $N = 20$ from 1000 unique spill episodes, each corresponding to a different random seed. The target is the corrected spill intensity s_{t+1}.

The model is trained using a combination of reconstruction loss and KL divergence over the posterior distribution of the latent variables:

$$\mathcal{L} = \frac{1}{T} \sum_{t=1}^{T} \left[\underbrace{\|\hat{s}_{t+1} - s_{t+1}\|_2^2}_{\text{Reco Loss}} \right. $$
$$\left. + \beta \cdot \underbrace{D_{\text{KL}}\left(q(z_{t+1} \mid s_{t+1}, a_t, h_t) \| p(z_{t+1} \mid h_t)\right)}_{\text{KL Divergence}} \right]$$

To ensure compatibility with our PID studies, training data is generated using log-normal noise with parameters $\mu = -0.347$ and $\sigma = 0.833$, and fixed PID gains: $G_p = -0.0101$, $G_i = -0.1897$, $G_d = -0.67678$.

The model uses a gated recurrent unit (GRU) to update hidden states h_t. At inference, we use a fixed history of $N = 20$ steps to predict the next 10 time steps, using only the first prediction. For the autoregressive model trained via teacher weaning, during inference we begin with a 20-step warmup of simulator produced inputs, after which predictions are made recursively by the surrogate interacting with the PID controller within the environment .

Results

Model Trained with Teacher Forcing   To assess stability, we evaluate 1-step prediction performance with an $N = 20$ simulator generated history for 100 unseen spills, each with a unique seed. Figure 1 shows the predictions for a given spill. We report mean absolute error (MAE) both point-wise and summed per spill, using 5 latent-space samples per point.
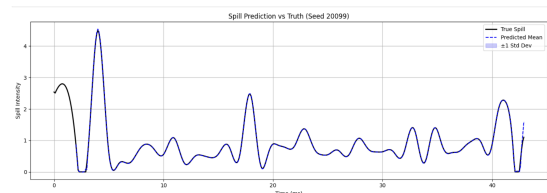

Figure 1: Sample predicted spill using a sliding window history of simulator truth trajectory $N = 20$ averaged over 5 samples from latent distribution.

We report relatively small MAE per spill given the scale of our data (Figures 2 and 3). To establish the uncertainty potential of this model, we also plot the model's standardized prediction errors (Figure 4) where μ_{pred} is the predicted spill at a timestep y_{true} is the simulator truth history and σ_{pred} is the predicted standard deviation at a timestep.

We see that the standardized σ of pointwise predicted errors is much greater than 1 implying some degree of under
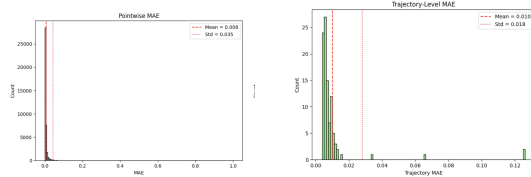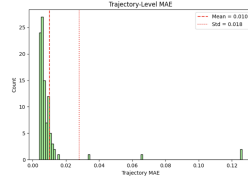
Figure 2: MAE per point.
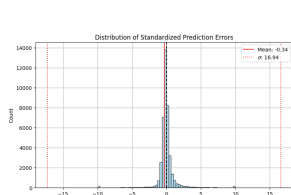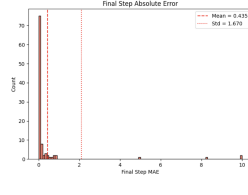

Figure 3: MAE per Trajectory

Figure 7: SDF of Surrogate Generated Spill trajectories over all seeds.

Figure 8: Wasserstein distance of surrogate trajectories over all seeds

Figure 4: In a perfect variational model, our mean should be 0, and $\sigma = 1$.

Figure 5: Final step absolute error per trajectory is much larger than the MAE per trajectory.

confident predictions. We additionally see that much of the error is located in the final step prediction per trajectory (Figure 5).

Autoregressive Model Trained with Teacher Weaning To evaluate our model, we sample 20 trajectories over 10 spills, each spill corresponding to a random seed. Upon initial observation, we find that though we have effectively modeled dynamics visually, some trajectories exhibit high divergence due to some compounding error. We filter the set of surrogate generated trajectories by keeping only those for which the third central moment difference satisfies $\mu_3^{\text{simulator}} - \mu_3^{\text{surrogate}} \geq -160$, thereby removing samples with large negative skewness discrepancies relative to the simulated spill. We show such trajectories in color for a given seed in Figure 6.
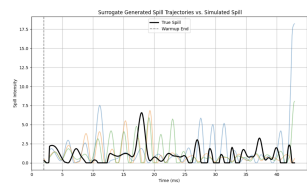

Figure 6: Surrogate spills generated after skew filter.

From the initial surrogate predictions, 31 of 200 trajectories remain after filtering. For these, we compute the Earth Mover's Distance (EMD) [7] between simulated and surrogate spills across all seeds, and compare the surrogate SDF to the corrected spill SDF from the simulator (Figures 7 and 8). While SDF values correlate at lower spill intensities, the surrogate generally produces lower SDFs than the simulator, likely due to end-of-trajectory divergence.

To stabilize spill predictions, we use confidence-weighted exponential smoothing. At each time step t, the model samples 5 predicted spill values $\{\hat{s}_t^{(i)}\}$, from which we compute a mean $\ha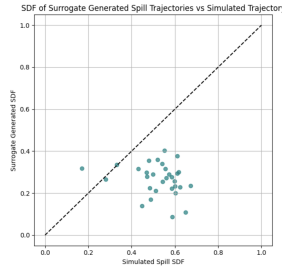t{\mu}_t$ and standard deviation $\hat{\sigma}_t$. We smooth the mean using an exponential moving average (EMA): $\text{EMA}_t = \lambda\hat{\mu}_t + (1 - \lambda)\text{EMA}_{t-1}$. Confidence is defined as $c_t = \exp(-\alpha\hat{\sigma}_t)$, decreasing with uncertainty. The final spill estimate is a confidence-weighted blend: $\tilde{s}_t = c_t \cdot \text{EMA}_t + (1 - c_t) \cdot s_{t-1}$, where the final result is clipped to be non-negative. This value $\tilde{s}_t$ is then used to compute the control action a_t for the given step during autoregressive inference. When using this procedure and making the same cut at $\mu_3^{\text{original}} - \mu_3^{\text{surrogate}} \geq -160$, we preserve 98 of the 200 trajectories. We similarly report the SDF correlation and Wasserstein distances for spills that pass this filter (Figures 9 and 10).
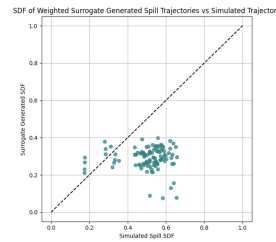

Figure 9: SDF of Surrogate Generated Spill trajectories vs. simulated spills with EMA filter and confidence weighting.
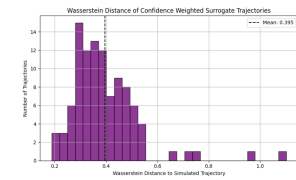

Figure 10: Wasserstein distance of surrogate trajectories to simulated spills with EMA filter and confidence weighting

We see initially that we are able to obtain less than extreme divergence of the surrogate generated spills from the simulator generated spills. The filtering and confidence weighting slightly improves this result with a lower mean Wasserstein distance. More statistics are needed to confirm this behavior.

CONCLUSION

We present an initial variational surrogate model for Mu2e slow spill dynamics. It shows early success in generating trajectories matching simulated spills, though SDF preservation needs improvement. Future work includes reducing reliance on filters, adding parameters to the loss function, and applying weighted re-sampling in the latent space to enhance performance, with the goal of integrating the surrogate into a differentiable RL control environment.

REFERENCES

[1] L. B. *et al.*, "Mu2e technical design report", 2015.
    doi:10.48550/arXiv.1501.05241

[2] J. A. Bistirlich, K. M. Crowe, A. S. L. Parsons, P. Skarek, and
    P. Truöl, "Photon spectra from radiative absorption of pions
    in nuclei", *Phys. Rev. C*, vol. 5, no. 6, pp. 1867–1883, 1972.
    doi:10.1103/PhysRevC.5.1867

[3] M. A. Ibrahim *et al.*, "Preliminary Design of Mu2E Spill Reg-
    ulation System (SRS)", in *Proc. IBIC'19*, Malmö, Sweden,
    Sep. 2019, pp. 177–180.
    doi:10.18429/JACoW-IBIC2019-MOPP033

[4] R. J. Williams and D. Zipser, "A learning algorithm for contin-
    ually running fully recurrent neural networks", *Neural comput.*,
    vol. 1, no. 2, pp. 270–280, 1989.

[5] S. Bengio, O. Vinyals, N. Jaitly, and N. Shazeer, "Scheduled
    sampling for sequence prediction with recurrent neural net-
    works", in *Advances in Neural Information Processing Systems
    (NeurIPS)*, 2015. doi:10.48550/arXiv.1506.03099

[6] D. P. Kingma and M. Welling, "Auto-encoding variational
    bayes", in *Proceedings of the 2nd International Conference
    on Learning Representations (ICLR)*, 2014.
    doi:10.48550/arXiv.1312.6114

[7] Y. Rubner, C. Tomasi, and L. J. Guibas, "A metric for distri-
    butions with applications to image databases", in *Proceedings
    of the Sixth International Conference on Computer Vision
    (ICCV)*, pp. 59–66, 1998.
    doi:10.1109/ICCV.1998.710701